This is the accepted manuscript made available via CHORUS. The article has been published as:

Dynamic polarizability of tungsten atoms reconstructed from fast electrical explosion of fine wires in vacuum

G. S. Sarkisov, S. E. Rosenthal, and K. W. Struve

Phys. Rev. A **94**, 042509 — Published 12 October 2016

DOI: 10.1103/PhysRevA.94.042509

Approved for FORMAL - Journal Article pursuant to US Government approval - SAND2016-1200 J
(tracking number - 397614)

Dynamic Polarizability of Tungsten Atoms Reconstructed from Fast Electrical Explosion of Fine Wires in Vacuum

G.S. Sarkisov

Raytheon Ktech, 10800 Gibson Blvd, Albuquerque, New Mexico, 87123, USA

S.E. Rosenthal and K.W. Struve

Sandia National Laboratories, Albuquerque, New Mexico, 87110, USA

Nanosecond electrical explosion of fine metal wires in vacuum generates calibrated, radially expanded gas cylinders of metal atoms surrounded by low-density fast expanding plasma corona. A novel integrated-phase technique, based on laser interferometry, provides the dynamic dipole polarizability of metal atoms. These data were previously unavailable for tungsten atoms. An extremely high melting temperature and significant pre-melt electronic emission make these measurements particularly complicated for this refractory metal. Most attempts to vaporize tungsten wire by electrical current pulse result in the disintegration of the sample into macro and micro fragments. However, application of a very fast rising current ~1 kA/ns can vaporize a thin 10-15 μm diameter tungsten wire and generate a calibrated gas-plasma cylinder. Adding a dielectric coating to the wire leads to increased energy deposition to the wire core and a reduction of the surrounding plasma corona. Employing the integrated-phase technique on a fast-exploding coated tungsten wire, we find that the dynamic dipole polarizability of tungsten atoms at a wavelength of 532 nm equals 15 ± 1.3 Å^3.

32.10.Dk, 52.70.Kz, 52.80.Qj

Approved for FORMAL - Journal Article pursuant to US Government approval - SAND2016-1200 J
(tracking number - 397614)

Introduction

Dipole polarizability is a fundamental atomic property. The static and dynamic dipole polarizabilities of atoms are required to obtain different atomic characteristics such as induced dipole moments, oscillator strengths, Stark and Kerr effects, Van der Waals constants and other characteristics related to the interaction of atoms with external electric fields [1-3]. Experimental data for dynamic and static polarizabilities for the metal atoms are very limited, and are mainly based on calculations [1-3]. In this paper, we present the first measurements of dynamic atomic polarizability for tungsten at a wavelength of 532 nm using our novel integrated-phase technique (IPh-technique) first proposed in [4].

The major problem for measurements of atomic polarizability for the metals is the controllable transformation of the initially solid substance into its gaseous state. This problem was successfully resolved in [4] using fast nanosecond electrical explosion of thin 10-20 μm diameter wires into vacuum. This technique permitted measurements of the dynamic atomic polarizability for a set of non-refractory metals Mg, Ag, Al, Cu and Au [4]. Under the influence of nanosecond-rising current, metal wire Joule heats and undergoes melting, surface vaporization of both metal and surface impurities, and finally, creates a hot plasma shell. Subsequently, heating stops in the central wire core due to rejection of the current from the core to the rapidly expanding, decreasingly resistive corona [5,6]. According to MHD simulations [6], the corona initially contains less than 1% of the wire mass. The remaining wire-core metal comprising the bulk of the original wire mass can be in a variety of conditions after corona generation: 1) vapor/plasma state, 2) liquid micro drops, 3) solid macro-fragments [5,7]. Vapor ionization most readily occurs when the vapor from hydrocarbon surface impurities is ionized by thermo-emitted electrons from the hot wire surface [7,8] before or during melting.

The main impediment to vaporizing tungsten in vacuum by an electrical pulse is the premature termination of the wire Joule heating due to rejection of the current from the wire core to the fast-expanding, low-density and low-resistive coronal plasma. This plasma formation, and the associated voltage breakdown, results from ionization of the surrounding vapor by thermo-electronic emission from the surface of the hot wire core [6,8]. An external radial electric field can affect the electronic emission by changing the potential barrier at the metal-vapor interface and leads to earlier or later breakdown, depending on the field direction [8]. This occurs because positive radial electric field (directed outward from the wire surface) increases the potential barrier for electronic emission (reduces electronic emission), while negative field reduces this barrier (increases the electronic emission). Hence, wire explosion with positive polarity allows the deposition of more energy to the wire core before breakdown than with negative polarity [8]. Moreover, positive-polarity explosion results in a "conical" energy deposition, where deposited energy into the wire core increases towards the high-voltage anode [8].

Tungsten is the refractory metal with the highest atomization enthalpy (~8.6 eV/atom) and strong electronic emission, particularly at the high temperatures that are possible with tungsten. Transformation of a tungsten wire core to any state from pre-melt disintegration to the totally vaporized state was first demonstrated in [7]. The complete transformation of 12 μm tungsten wire with a 2 μm dielectric coating into the plasma state during 3-5 ns of Joule heating was clearly demonstrated in [9]. In our paper we will show how corona-free explosion of the dielectric coated W wire [9] helps to measure dynamic atomic polarizability of the tungsten atoms.

Experimental Setup

The experimental setup is based on a high-voltage trigger generator MAXWELL TG-70 (0.1 μF capacitor with SF_6 gas switch, charging voltage up to 70 kV). The schematic of the coaxial target unit and vacuum chamber is presented in Fig. 1. The trigger generator was connected to the coaxial target unit via 7 m of RG-218 cable. Current and voltage were measured with a 1.2 GHz bandwidth coaxial CVR 1M-T10 and a fast V-dot (inductive coil monitor). The vacuum chamber was evacuated to 10^{-4} torr pressure to avoid air breakdown. All waveforms were captured by a Tektronix TDS5104B 1 GHz 4-channel digital oscilloscope. The tungsten wire, 5-10 mm length and 10-20 μm diameter, was placed in the center of the coaxial target unit inside the vacuum chamber. The pulser produced current though the wire at the rate of 1-1.5 KA/ns which is sufficient for its total vaporization [9].

Figure 1. Vacuum chamber with coaxial target unit.

Figure 2. Laser diagnostic setup.

Figure 2 shows the optical diagnostic setup. A short-pulse laser (EKSPLA SL312, 100 mJ, 532 nm, 150 ps, 1 ns jitter) was used for backlighting interferometry, shadowgraphy and schlieren diagnostics. A shearing air-wedge interferometer [10] was utilized to obtain the interferogram and shadowgram on the same camera. To reduce optical aberration the angle plane of the glass-wedge was adjusted orthogonal to the beam-splitting plane. The schlieren branch makes use of a radial knife-edge technique that produces separate areas of the schlieren image for gas-type refractivity (refractive index, μ > 1) and plasma refractivity (μ < 1) [11]. Fast 1 ns-rise time PIN-diode DET10A with 1 mm core optical fiber and collecting collimator captured light emission from the exploding wire.

Experimental Technique

It was shown in [4] that for a wire totally transformed into its gaseous state the radial integral of the interference phase-shift is proportional to the lineal density of the wire. The state of the expanding wire core depends on the amount of deposited energy. The more energy we deposit into the wire core, the greater its expansion velocity. The state of the expanding wire core varies with deposited energy from 1) liquid micro drops/clusters/gas, to 2) gas, to 3) gas/plasma, and finally to 4) the full plasma state. The radial integral of the interference phase-shift reaches a maximum positive value where the wire core has fully reached its gaseous state. As deposited energy (or expansion velocity) increases beyond the level associated with the complete gaseous state of the wire core, the phase integral drops to zero due to the growing density of free electrons, which produce a refractive index, μ < 1, as opposed to the refractivity of the atoms (bound electrons) μ > 1 [9]. The negative phase-shift grows with the degree of ionization and can thus significantly exceed the positive contribution from the neutral atoms. Our experimental goal then is to determine the maximum positive interference phase-shift radial integral vs expansion velocity in order to reconstruct the dynamic polarizability of the metallic atoms.

The expression for recovering the average dynamic dipole polarizability $\alpha(\lambda)$ at wavelength λ can be written as [4]:

$$\alpha(\lambda) = \frac{\lambda}{2\pi N_{lin}} \int \delta(y)dy \tag{1}$$

where α- is the polarizability in cm^3, λ- is the wavelength in cm, N_{lin} the lineal density of atoms in the wire in cm^{-1}, δ- is the interference phase-shift in fringes, and y- the probing path in cm in the direction perpendicular to the wire axis. Recovering the maximum polarizability vs. expansion velocity allows the measurement of dynamic atomic polarizability for the metal under investigation. This IPh-technique does not require axial symmetry of the expanding gas column; we simply assume that the wire expands in the radial direction and the lineal density of expanding mass is invariant value. Probing time should be at the moment when the expanding wire core becomes transparent to the probing laser. Probing at a later time results in the underestimation of the polarizability due to an apparent loss of detectable wire mass by interferometry.

Figure 3. Current, voltage and light waveforms with power and simulated voltage.

Experimental Results

Figure 3 displays current, voltage, light emission, power, and ThD simulated voltage (thermo-dynamic simulation using temperature-dependent resistivity and heat capacitance data for the metal) [12] waveforms for an exploding 11.5 μm diameter W wire with 5.5 mm length (shot 012607-1). The wire has a polyamide coating of 2 μm thickness to prevent early breakdown and premature termination of Joule heating of the wire core. Charging voltage was 45 kV (60% of maximum value). The voltage reached a maximum ~58 kV during the first ~6 ns and then collapse to zero with a subsequent oscillation phase. Voltage collapse is related to the generation of a plasma shell around the hot wire due to ionization of the vaporized hydrocarbon impurities on the wire surface during Joule-heating. The hot plasma shell (~100 eV) expands rapidly into the vacuum (~100 km/s). The plasma resistivity exceeds that of the heated wire core; however, the expanding plasma shell geometrically provides a much lower-impedance path for the current than the wire core, switching the current out of the core, and dropping the cathode-anode resistance, resulting in a collapse of the voltage. The high voltage spike has only ~4 ns width at half amplitude. A simple thermo dynamical calculation [12] of wire heating demonstrates reasonable agreement with the experimental resistive voltage up to melt time. According to the ThD-calculation W-wire melting starts at 46 kV (t~0 ns). The amount of deposited Joule energy is ~0.44 J (~76 eV/atom, ~40 kJ/g). This deposited energy corresponds to ~9 times the atomization enthalpy for tungsten (8.6 eV/atom) and should fully transform the W wire core into the plasma state. The period leading up to this transformation provides ample opportunity to probe the wire core during its fully gaseous state.

Figure 4. Interferogram, shadowgram and schlieren images of an exploding W wire at 60 ns.

Figure 4 presents interferogram, shadowgram and schlieren images, simultaneously taken at 60 ns after the start of the current. The anode is at the top of the images. The schlieren image shows a spark of the probing light intensity close to both the cathode and anode on the right side of the wire axis, corresponding to gas-type refractivity. For the mid-anode-cathode-gap, or central portion of the wire, which expands faster, we observe a light spark on the left side of the wire axis corresponding to plasma-type refractivity. Compression of the interference lines on the right side of the wire axis and decompression on the left side at electrode areas also point out a gas-type refractivity. The shadowgram exhibits increases of wire expansion from either electrodes to the central region, which is nearly cylindrical and homogenous. This wire expansion cone is similar to what was observed for bare wires due to the polarity-effect [8]. The sign and amplitude of the radial electric field determines the level of energy deposited into the wire core before voltage breakdown [8].

Figure 5. Radial profiles of phase-shits at different cross-sections.

Figure 5 shows a set of radial profiles of the interference phase-shift at different cross-sections Z1-Z4. We can see the positive gas-type phase-shift in the Z1-Z2 cross-sections, dropping to almost zero at Z3 and finally to the negative plasma-type phase-shift in Z4. According to the integrated-phase technique discussed above, the positive maximum of the phase-shift integral gives the atomic polarizability of the metal atoms.

Figure 6 demonstrates the radial phase-shift for the cross-section at Z=1.44 mm above the cathode (ground) holder. The integral of the phase-shift was calculated from the smooth interpolated curve and gives a polarizability value of ~14.9 Å^3. The expansion velocity was determined from the phase-shift curve to be ~8.2 km/sec.

Figure 6. Radial profile of phase-shift corresponding to the gas stage of exploding W wire.

Figure 7 shows the axial distribution of the reconstructed polarizability using equation (1) and the expansion velocity. While expansion velocity increases monotonically with distance from the cathode to about mid-gap, the reconstructed polarizability initially increases with distance, reaching its maximum value of ~15 Å^3 close to the cathode at 1.4-1.9 mm, drops to zero at 2.8 mm and becomes negative above 2.8 mm mid-gap. Only the maximum positive reconstructed polarizability has the physical meaning of "dynamic atomic polarizability" at the probing wavelength, 532 nm.

At Z=1.4-1.9 mm, where the wire reaches its gaseous state, the wire expansion stops increasing. Above Z=1.9 mm the expansion starts to rise again, where the reconstructed polarizability begins falling. The expansion-plateau at gas-state area is an interesting phenomenon. Probably it is related to different electron-emission property of the wire core under different state.

Figure 7. Axial distribution of polarizability and velocity for exploding 11.5 μm W wire overlapped with corresponding part of shadowgram image.

Figure 8. Statistical distribution of the reconstructed polarizability for W vs. expansion velocity.

Figure 8 shows the reconstructed polarizability vs expansion velocity of the wire core, obtained from three different experiments. All wires were 11.5 μm diameter and 5.5 mm length, W with 2 μm thick polyamide-coating, and the probing time was either 60 ns or 80 ns after the current starts. We can see statistically similar behavior for all wires: the reconstructed polarizability grows from ~8 Å^3 up to ~15±1.3 Å^3 when the expansion velocity increases from 5 to 8 km/sec. Above 8 km/sec the reconstructed polarizability drops to zero at ~14 km/s and becomes negative. It is interesting that, consistent with Fig. 7 for a single shot, tungsten totally transforms to its gaseous state when the expansion velocity reaches ~8 km/s.

Conclusion.

We demonstrate the first measurement of dynamic dipole polarizability of tungsten atoms at a wavelength of 532 nm. Tungsten is a refractory metal, with high melting temperature ~3680

K (second only to carbon at 3773 K) and the greatest atomization enthalpy ~8.6 eV/atom among all of the elements of the Periodic Table. Most attempts to vaporize this metal in vacuum with an electrical pulse result in a pre-melt breakdown and associated cessation of Joule heating of the wire core. However, application of a fast-rising current ~1 kA/ns allows energy deposition sufficient for the transformation of a bare W wire into its liquid-vapor state [7]. For W wire with a polyamide dielectric coating and fast-rising current, we can transform W into its gas-plasma state [9] and generate a well-characterized expanding gas cylinder. Increasing the energy deposition from the cathode wire holder to the central region of the wire by exploiting the radial electric field polarity effect, allows the generation of different states of metal along the wire axis. Because the exploding wire expands in the radial direction, the lineal density of the expanding W cylinder remains constant. Using the integrated-phase technique, we are able to reconstruct the dynamic dipole polarizability of tungsten atoms at a wavelength of 532 nm as 15±1.3 $Å^3$. The main sources of error reside in the measurements of the interference phase-shift (±0.1 line) and the wire diameter (±0.5 μm). Measurement error can be estimated as 8-10%.

Acknowledgement

Sandia is a multiprogram laboratory operated by Sandia Corporation, a Lockheed Martin Company, for the National Nuclear Security Administration under DE-AC04-94AL85000.

Reference:

1. T. M. Miller and B. Bederson, Adv. At. Mol. Phys. **25**, 37 (1988).
2. K. D. Bonin and M. A. Kadar-Kalen, Int. J. Mod. Phys. B **8**, 3313 (1994).
3. J. Mitroy, M. S. Safronova, C. W. Clark, J. Phys. B 43, 202001 (2010).
4. G. S. Sarkisov, I. L. Beigman, et al., Phys. Rev. A **73**, 042501 (2006).
5. S. V. Lebedev and A. I. Savvatimskii, Sov. Phys. Uspekhi **27**, 749 (1984).
6. G. S. Sarkisov, S. E. Rosenthal, K. R. Cochrane, et al., Physical Review E **71**, 046404 (2005).
7. G. S. Sarkisov, K. W. Struve, and D. H. McDaniel, Physics of Plasmas **12**, 052702 (2005).
8. G. S. Sarkisov, P. V. Sasorov, K. W. Struve, et al., Physical Review E **66**, 46413 (2002).
9. G. S. Sarkisov, S. E. Rosenthal, K. W. Struve, et al., Physical Review E **77**, 056406 (2008).
10. G. S. Sarkisov, Instrum. Exp. Tech. **39**, 5, 727 (1996); (https://en.wikipedia.org/wiki/Air-wedge_shearing_interferometer).
11. L. A. Vasil'ev, *Schlieren Methods* (KETER Inc., New York, 1971), p. 25.
12. G. S. Sarkisov, S. E. Rosenthal, and K. W. Struve, Rev. Sci. Instrum., **78**, 033503 (2007).

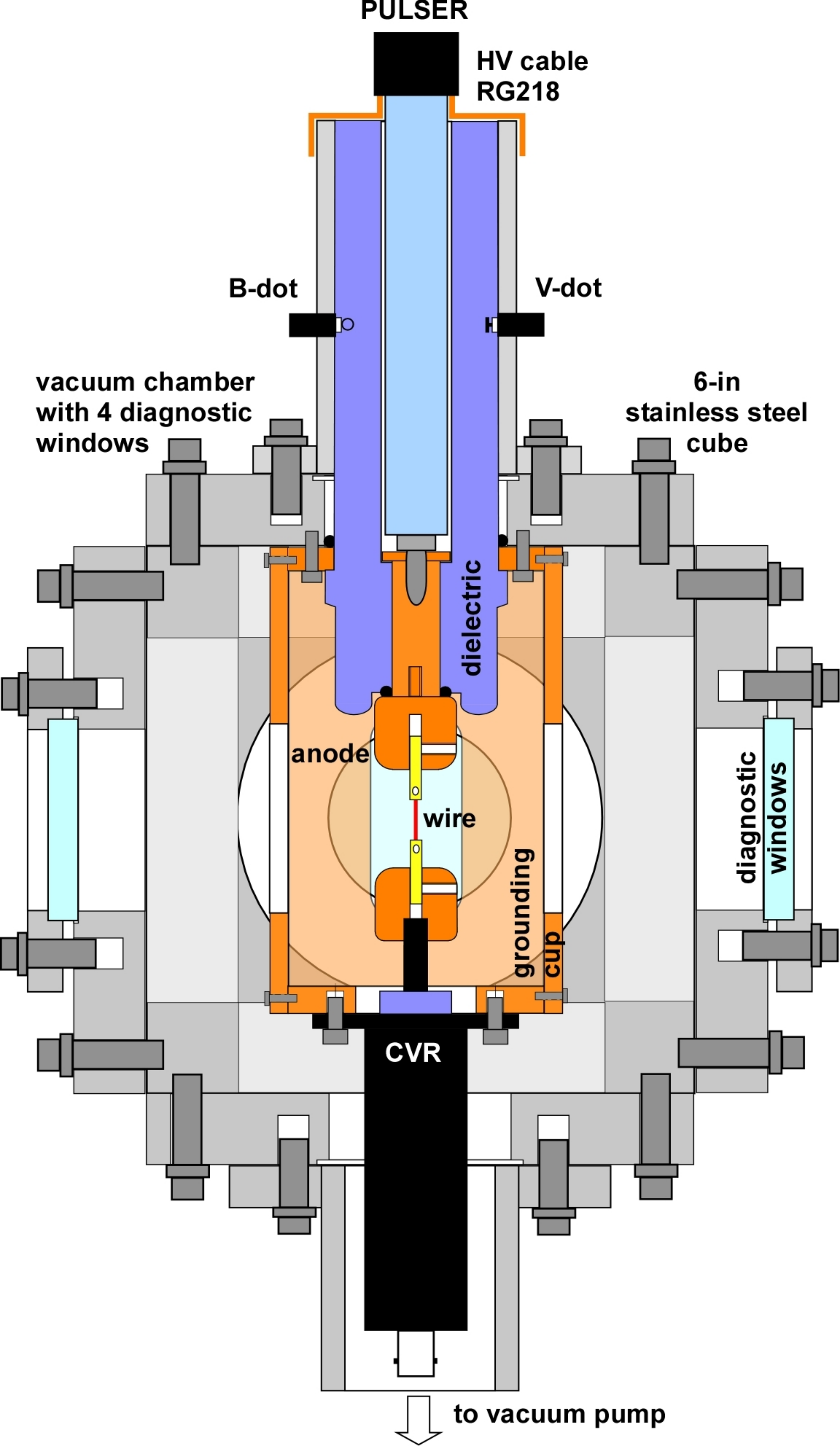
PULSER
HV cable
RG218
B-dot
V-dot
vacuum chamber
with 4 diagnostic
windows
6-in
stainless steel
cube
dielectric
anode
wire
grounding
cup
diagnostic
windows
CVR
to vacuum pump

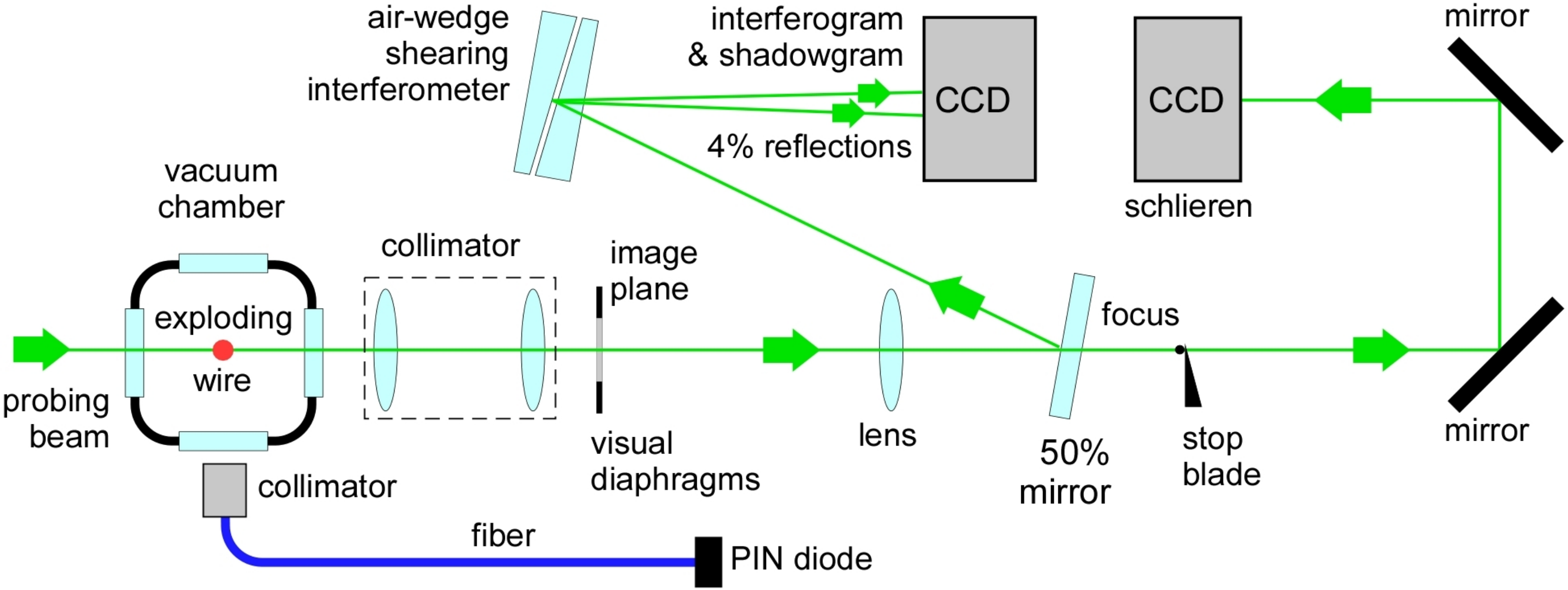
air-wedge shearing interferometer
interferogram & shadowgram
CCD
CCD
mirror
4% reflections
schlieren
vacuum chamber
collimator
image plane
focus
exploding
wire
probing beam
lens
50% mirror
stop blade
mirror
visual diaphragms
collimator
fiber
PIN diode

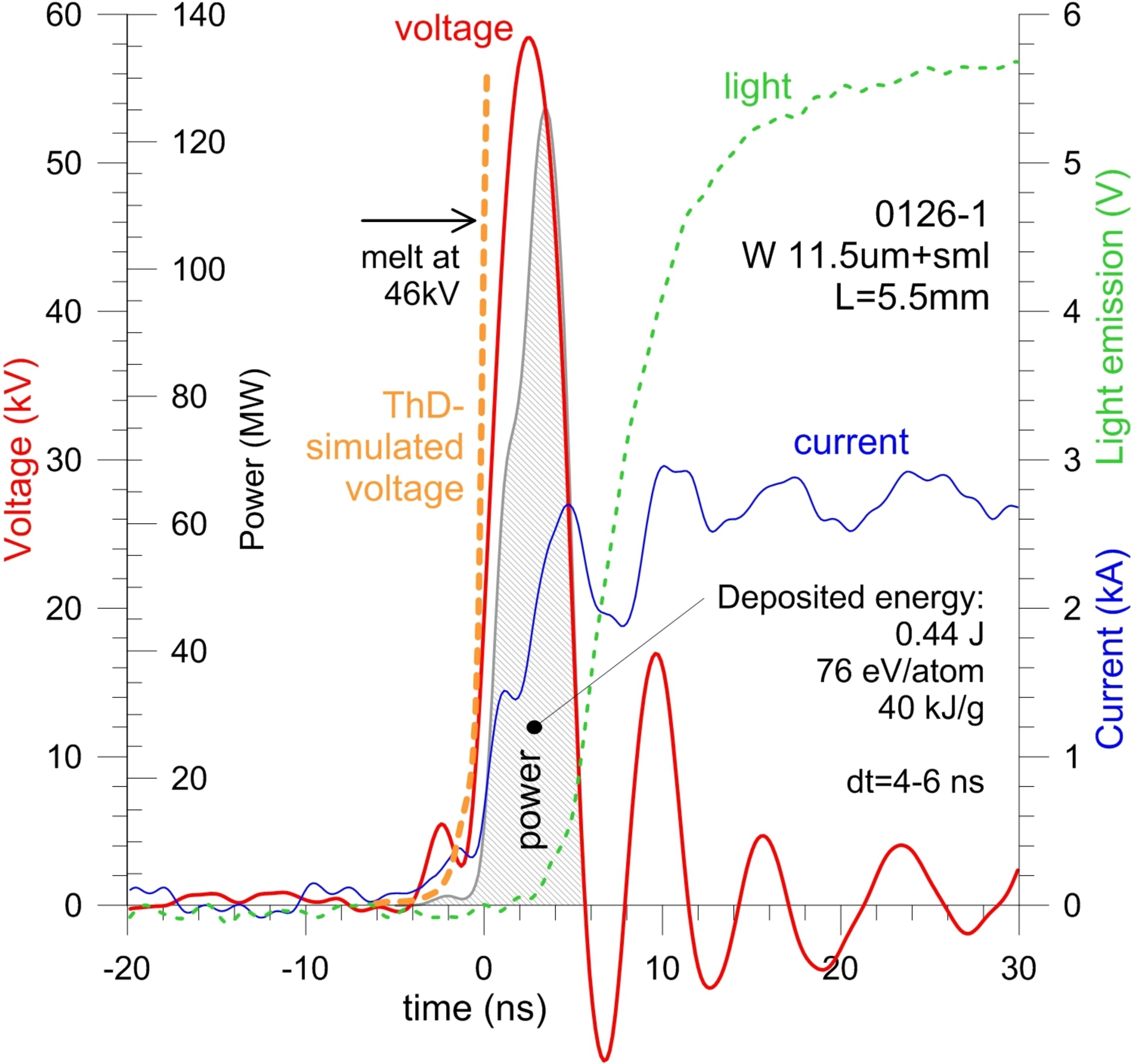
voltage
light
melt at
46kV
ThD-
simulated
voltage
0126-1
W 11.5um+sml
L=5.5mm
current
Deposited energy:
0.44 J
76 eV/atom
40 kJ/g
dt=4-6 ns
power
Voltage (kV)
Power (MW)
Light emission (V)
Current (kA)
time (ns)
0
10
20
30
40
50
60
20
40
60
80
100
120
140
0
1
2
3
4
5
6
-20
-10
0
10
20
30

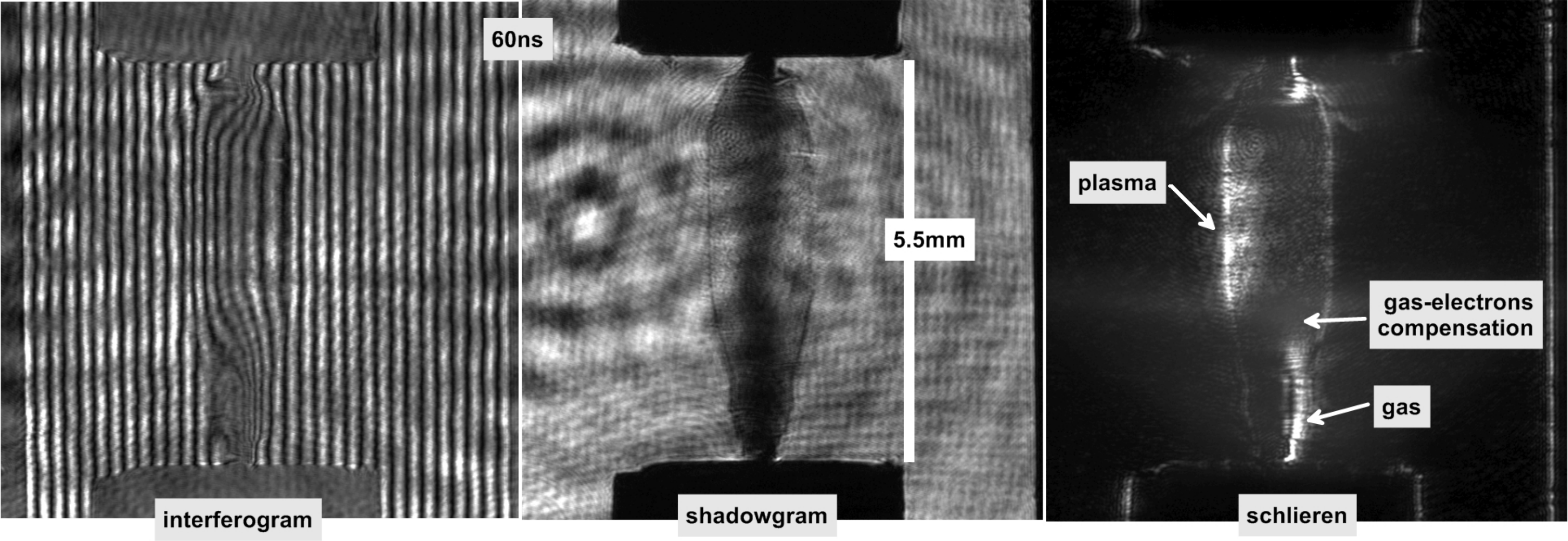
60ns
interferogram
shadowgram
5.5mm
plasma
gas-electrons compensation
gas
schlieren

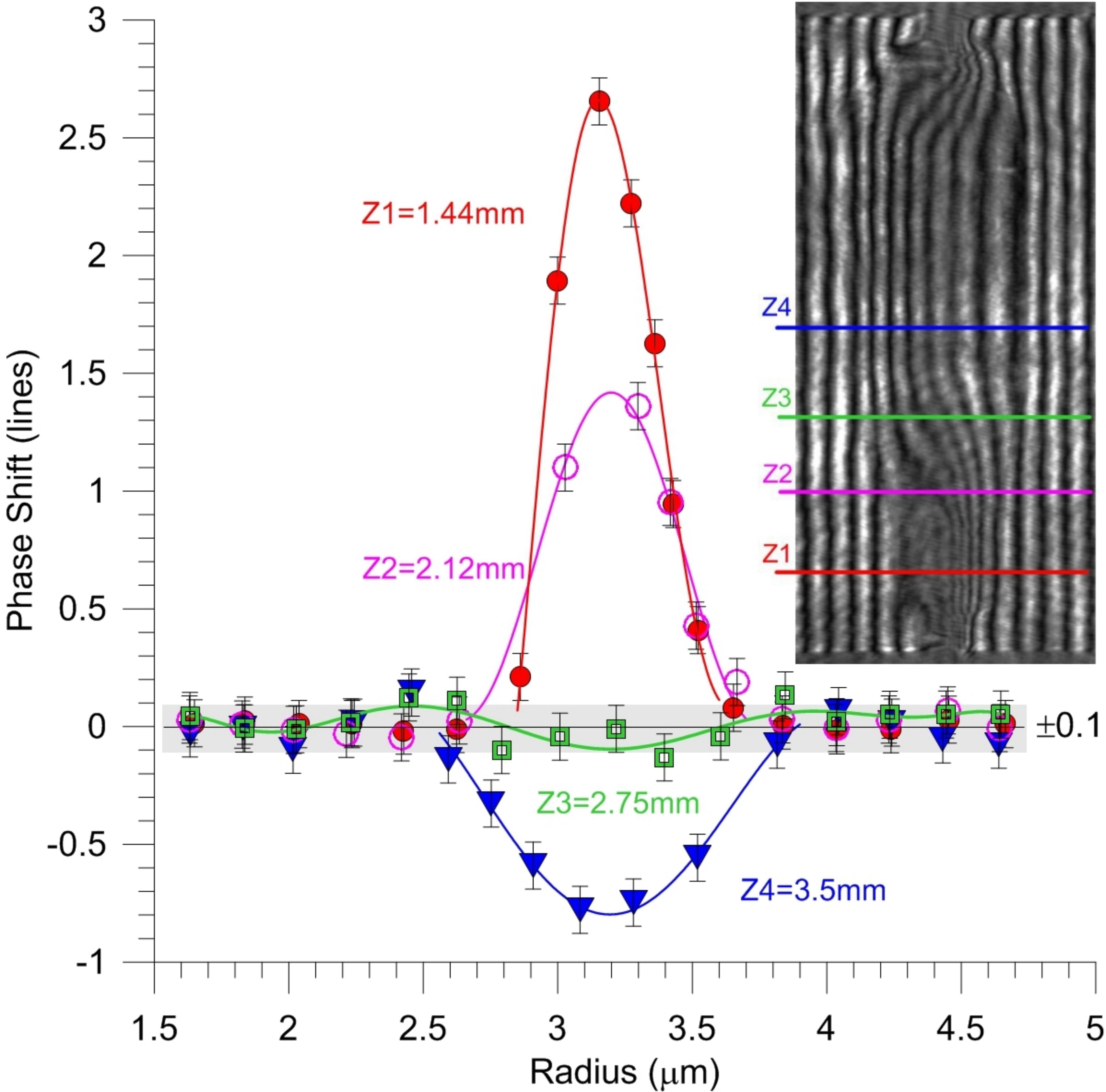
Phase Shift (lines)
Radius (μm)
3
2.5
2
1.5
1
0.5
0
-0.5
-1
1.5
2
2.5
3
3.5
4
4.5
5
Z1=1.44mm
Z2=2.12mm
Z3=2.75mm
Z4=3.5mm
±0.1
Z4
Z3
Z2
Z1

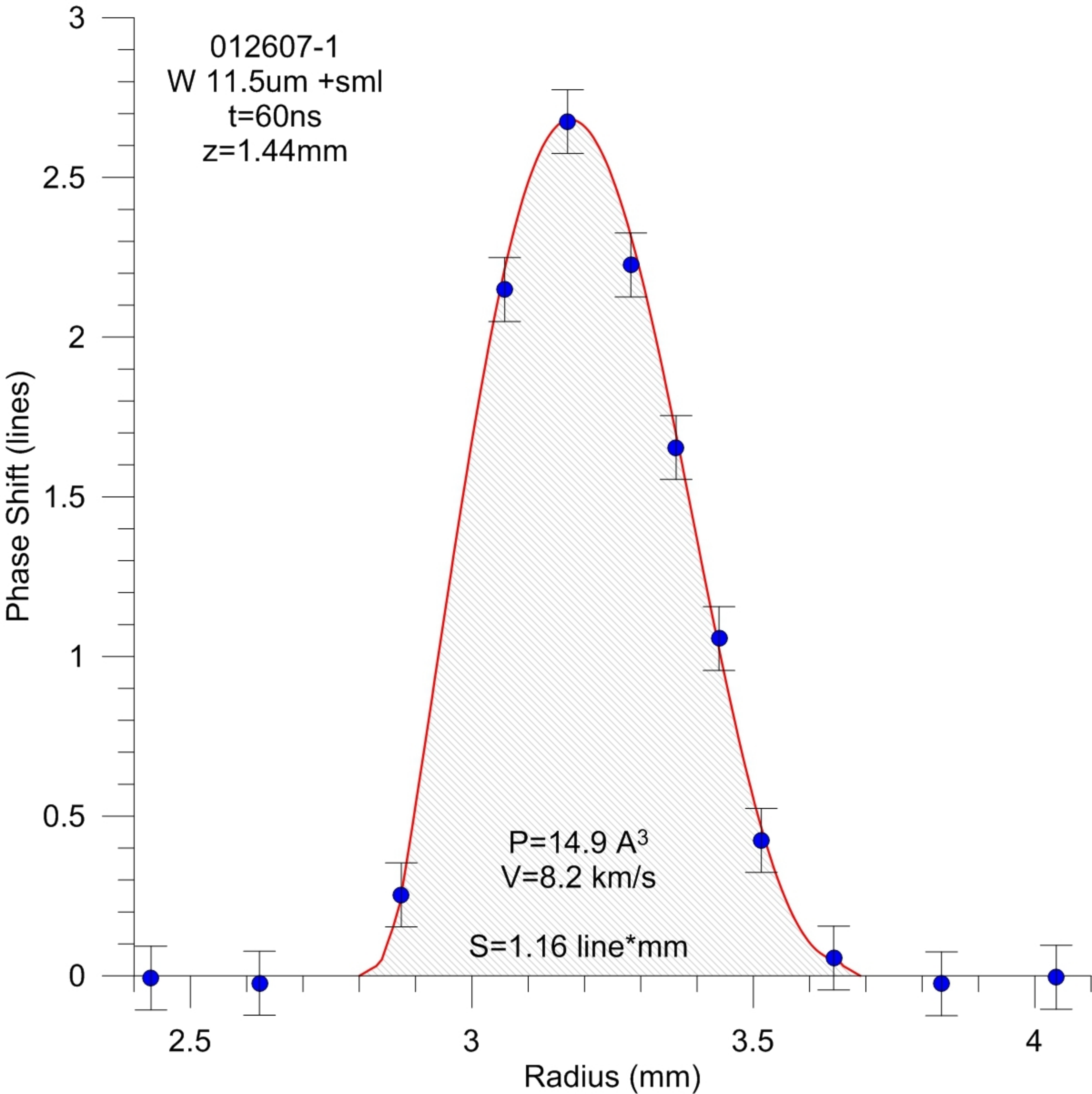
012607-1
W 11.5um +sml
t=60ns
z=1.44mm
P=14.9 A³
V=8.2 km/s
S=1.16 line*mm
Phase Shift (lines)
Radius (mm)
3
2.5
2
1.5
1
0.5
0
2.5
3
3.5
4

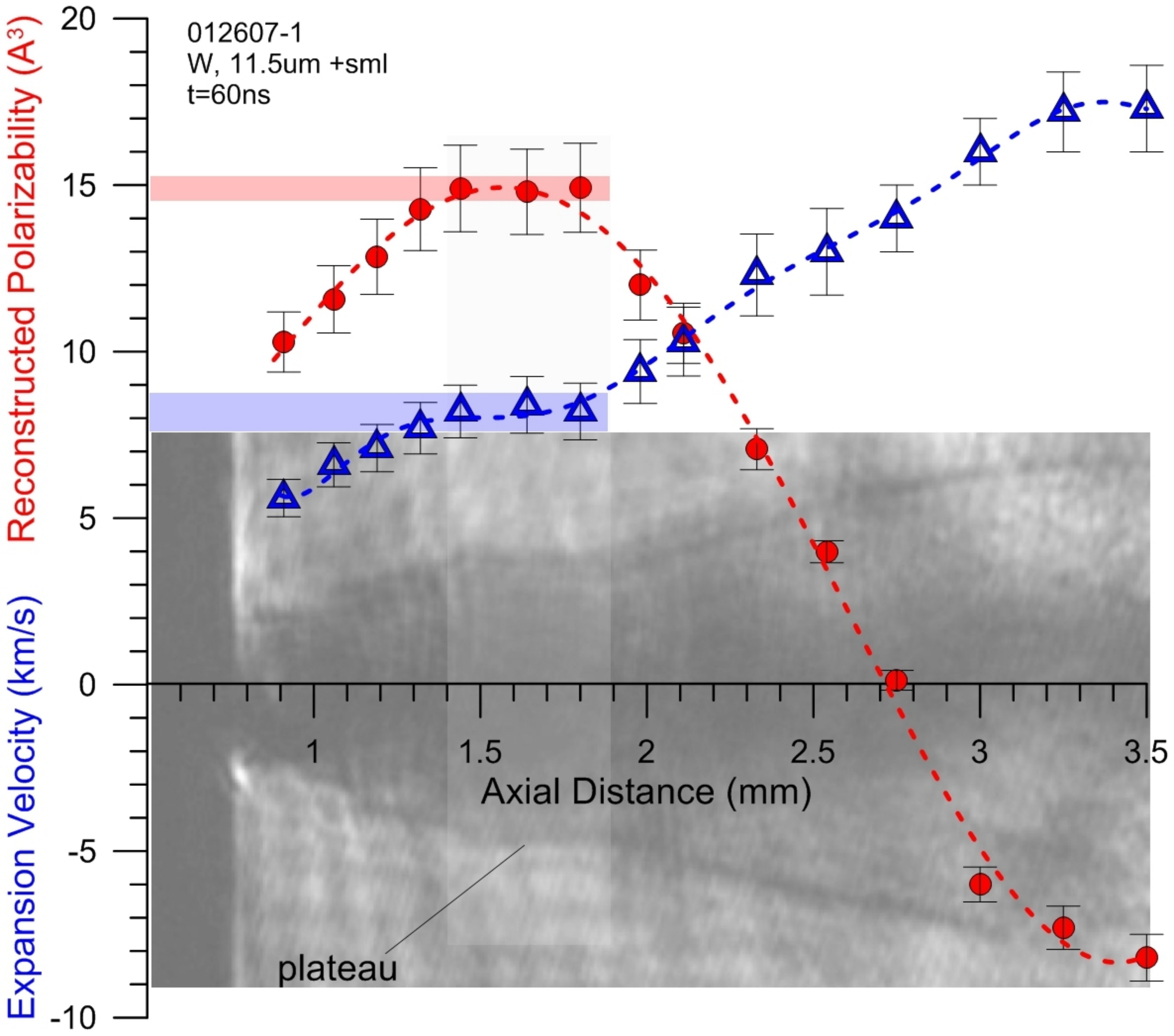
012607-1
W, 11.5um +sml
t=60ns
Reconstructed Polarizability (A^3)
Expansion Velocity (km/s)
20
15
10
5
0
-5
-10
1
1.5
2
2.5
3
3.5
Axial Distance (mm)
plateau

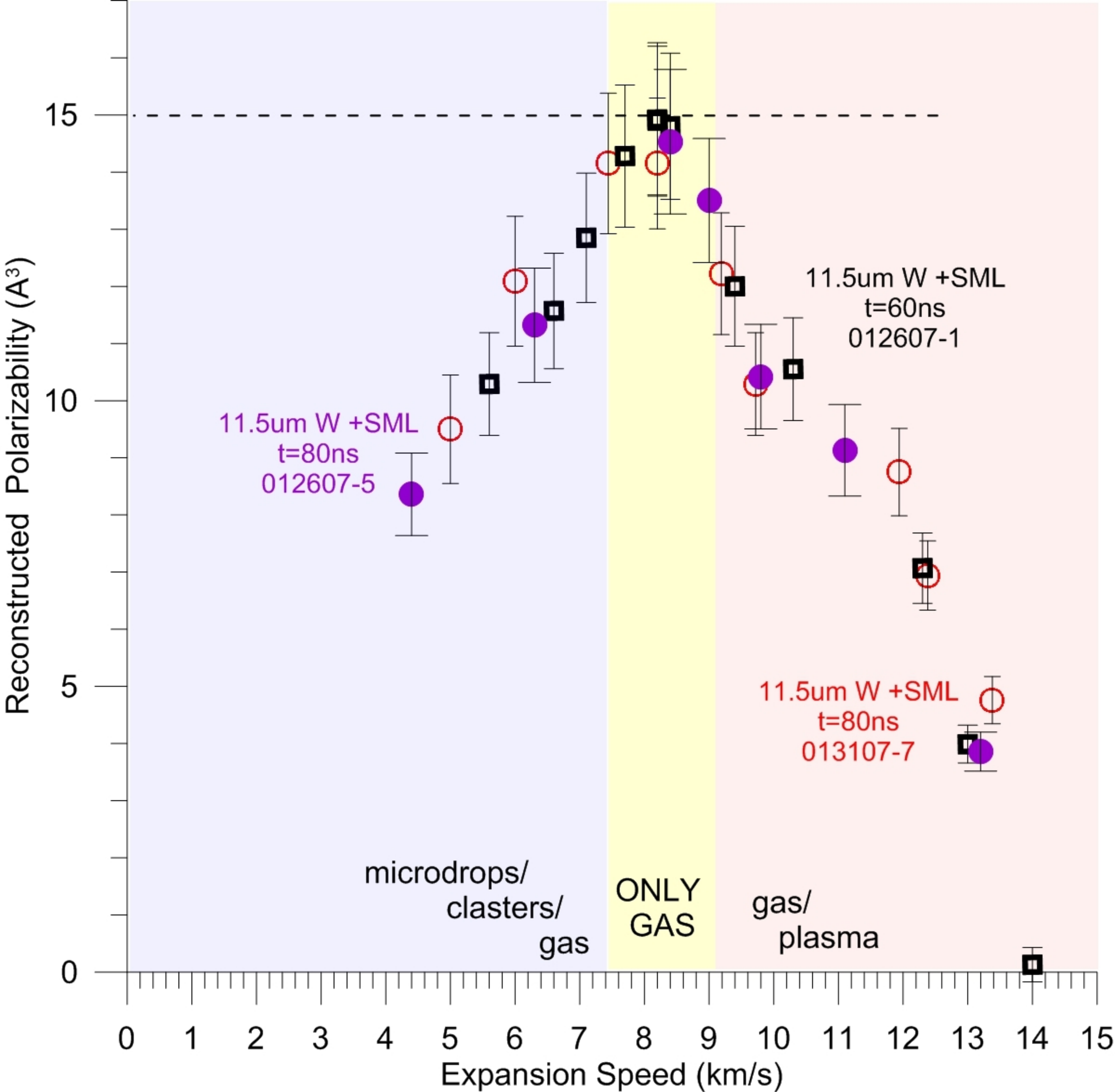
Reconstructed Polarizability (A^3)
Expansion Speed (km/s)
0
5
10
15
0
1
2
3
4
5
6
7
8
9
10
11
12
13
14
15
11.5um W +SML
t=80ns
012607-5
11.5um W +SML
t=60ns
012607-1
11.5um W +SML
t=80ns
013107-7
microdrops/
clasters/
gas
ONLY
GAS
gas/
plasma